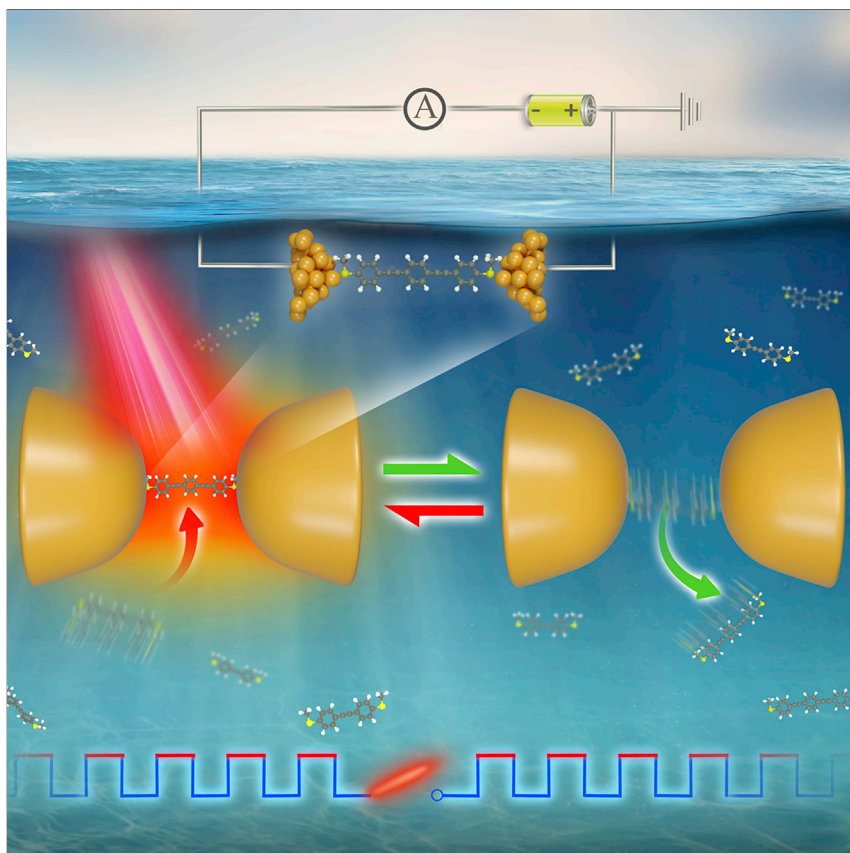


## Article

## Single-Molecule Plasmonic Optical Trapping



We develop a strategy to directly trap, investigate, and release single molecules ( $\sim 2$  nm) in solution by using an adjustable plasmonic optical nanogap, which opens an avenue to manipulate single molecules and other objects in the size range of primary interest for physics, chemistry, and life and material sciences without the limitations of strong bonding group, ultra-high vacuum, and ultra-low temperature, and makes possible controllable single-molecule manipulation and investigation as well as bottom-up construction of nanodevices and molecular machines.

Chao Zhan, Gan Wang, Jun Yi, ..., Yang Yang, Wenjing Hong, Zhong-Qun Tian

yangyang@xmu.edu.cn (Y.Y.)

whong@xmu.edu.cn (W.H.)

zqtian@xmu.edu.cn (Z.-Q.T.)

**HIGHLIGHTS**

Directly trap, investigate, and release single molecules by plasmonic optical nanogap

Push the volume of a free object that can be manipulated in solution down to  $\sim 2$  nm

The trapping force originates from plasmonic nanomaterials under illumination

**Demonstrate**

Proof-of-concept of performance with intended application/response

Zhan et al., Matter 3, 1350–1360

October 7, 2020 © 2020 Published by Elsevier Inc.

<https://doi.org/10.1016/j.matt.2020.07.019>



## Article

## Single-Molecule Plasmonic Optical Trapping

Chao Zhan,<sup>1,2</sup> Gan Wang,<sup>1,2</sup> Jun Yi,<sup>1,2</sup> Jun-Ying Wei,<sup>1</sup> Zhi-Hao Li,<sup>1</sup> Zhao-Bin Chen,<sup>1</sup> Jia Shi,<sup>1</sup> Yang Yang,<sup>1,\*</sup> Wenjing Hong,<sup>1,\*</sup> and Zhong-Qun Tian<sup>1,3,\*</sup>

## SUMMARY

The volume of the object that can be manipulated in solution is continuously decreasing toward an ultimate goal of a single molecule. However, Brownian motions suppress the molecular trapping. To date, free-molecule trapping in solution has not been accomplished. Here, we develop a strategy to directly trap, investigate, and release single molecules (~2 nm) in solution by using an adjustable plasmonic optical nanogap, which has been further applied for selective single-molecule trapping. Comprehensive experiments and theoretical simulations demonstrated that the trapping force originated from plasmonic nanomaterials. This technique opens an avenue to manipulate single molecules and other objects in the size range of primary interest for physics, chemistry, and life and material sciences without the limitations of strong bonding group, ultra-high vacuum, and ultra-low temperature, and makes possible controllable single-molecule manipulation and investigation as well as bottom-up construction of nanodevices and molecular machines.

## INTRODUCTION

The manipulation of free molecules is critical for investigating single-molecule processes in physics, chemistry, and material and life sciences, as well as construction of nanodevices and molecular machines. However, molecular trapping is strongly suppressed by Brownian motions. Three strategies have been developed to trap single molecules. One strategy is to bind molecules to microstructures to scale up trapping forces and then manipulate them using optical tweezers,<sup>1–4</sup> magnetic tweezers,<sup>5,6</sup> or a scanning probe microscope<sup>7,8</sup>, which is greatly limited by strong interactions between molecules and microstructures while it is challenging to achieve controllable trapping and release. Another strategy is based on laser cooling in an ultra-high vacuum (UHV) condition to reduce thermal fluctuations,<sup>9,10</sup> which has been used to directly trap cesium dimer and strontium monofluoride.<sup>11,12</sup> However, it is difficult to extend this technique to more complex molecules, and the required UHV system limits its applications. The third approach, anti-Brownian electrokinetic (ABEL) trapping, was also able to overcome Brownian motion in a 2D plane by combining a fast detection scheme with real-time feedback. However, the molecules trapped by an ABEL trap should be fluorescent and are randomly moving in an area of several hundreds of nanometers.<sup>13,14</sup> Until now, the trapping of a free object with a size of several nanometers in solution has remained a major challenge. It is highly desirable to develop a method to trap free single molecules directly (Supplemental Information shows the main techniques currently used for single-molecule manipulation and the evolution of optical trapping, Figures S1 and S2).

Optical trapping is a promising way to achieve this goal. Since the first report of the use of optical force to trap micrometer-sized materials in 1970,<sup>1</sup> it has been

## Progress and Potential

The volume of the object that can be trapped in solution has been continuously pushed toward an ultimate goal of the single-molecule level over the past 50 years, and is considered as the key step for investigating single-molecule processes as well as construction of nanodevices and molecular machines. However, until now no technique has been able to achieve this goal due to the significant Brownian motions. Here, we demonstrate that a free single molecule of ~2 nm can be directly trapped, investigated, and released in solution using plasmonic nanomaterials, pushing the volume of a free object that can be manipulated in solution down to an unprecedented 2 nm, thus offering an approach for the trapping of single molecules or other objects in the size range of primary interest to physics, chemistry, and life and material sciences without the limitations of strong bonding group, ultra-high vacuum, and ultra-low temperature.

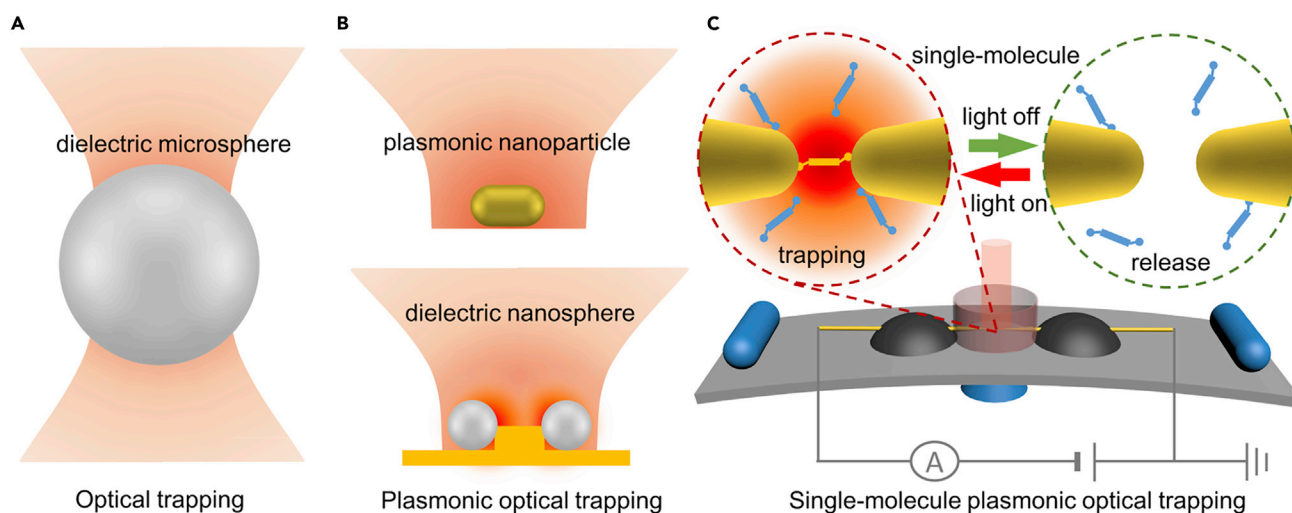


**Figure 1. Schematic of Direct Single-Molecule Plasmonic Optical Trapping Compared with Other Optical Trapping Methods**

(A) Conventional optical trapping relies on the field gradients near the focus of a laser beam and are commonly used for trapping microspheres. (B) Plasmonic optical trapping is based on the enhanced electromagnetic field by SPs and have two typical modes: one mode is using the focused laser to trap plasmonic nanoparticles while the other mode is using the plasmonic nanostructure to trap dielectric nanoparticles. (C) Single-molecule plasmonic optical trapping is composed of two gold nanotips under illumination to provide a substantial localized electromagnetic field due to the SP effect. During the single-molecule trapping experiments, the tunneling current through the nanogap is measured by a lab-built mechanically controllable break junction with high mechanical stability. Two laser beams (514 nm, 691 nm) were used to match the interband transition and surface plasmon resonance, respectively. The setup allows us to change the wavelength, polarization, and intensity of the incident light. The default light intensity is 50 mW ( $\sim 10^6$  W/m<sup>2</sup>).

commonly used to manipulate dielectric microspheres, single cells, or other objects (Figure 1A).<sup>6,15–18</sup> However, conventional optical trapping, which depends on the field gradients near a focused laser beam, have a diffraction-limited trapping volume.<sup>1,19–21</sup> Around the year 2000, through theoretical simulations, several groups proposed to trap nanosized particles, and even single molecules, based on the enhanced electromagnetic field by surface plasmons (SPs), which offers an opportunity to overcome the diffraction limit of conventional optical trapping.<sup>22–24</sup> Soon afterward, plasmonic optical trapping was experimentally demonstrated to trap particles with sub-wavelength volumes (10–250 nm), including trapping dielectric nanoparticles with the assistance of a plasmonic nanostructure<sup>25–28</sup> and trapping plasmonic nanoparticles in diffraction-limited laser beams (Figures 1B and S2).<sup>29–31</sup> Plasmonic optical trapping was then extended to filtrate dielectric particles with different dimensions,<sup>32</sup> trap proteins,<sup>33,34</sup> generate enantioselective optical forces,<sup>35</sup> drive a nanorotary motor,<sup>36</sup> and trap a gold nanoparticle in a plasmonic nanohole for single-molecule detection.<sup>37</sup> Using surface enhanced single-molecule spectroscopy, several previous works also emphasized the effects of plasmonic optical trapping.<sup>23,38</sup> However, the ultimate goal of directly trapping single chemical molecules has not yet been accomplished. According to theoretical investigations, a localized and sufficient optical force, arising from an electromagnetic field gradient, is required to overcome the Brownian motions.<sup>22–24,39</sup> Moreover, an *in situ* single-molecule identification technique is essential to detect single-molecule trapping events.

Here, we achieved direct single-molecule ( $\sim 2$  nm) optical trapping and release in solution using two coupled plasmonic nanotips controlled by a mechanically controllable break junction setup,<sup>40–43</sup> which supplies a strong electric field in the gap under illumination wherein the individual molecule is trapped. Meanwhile, the

<sup>1</sup>State Key Laboratory of Physical Chemistry of Solid Surfaces, Collaborative Innovation Center of Chemistry for Energy Materials (iChEM), College of Chemistry and Chemical Engineering, Pen-Tung Sah Institute of Micro-Nano Science and Technology, Xiamen University, Xiamen 361005, China

<sup>2</sup>These authors contributed equally

<sup>3</sup>Lead Contact

\*Correspondence: yangyang@xmu.edu.cn (Y.Y.), whong@xmu.edu.cn (W.H.), zqtian@xmu.edu.cn (Z.-Q.T.)

<https://doi.org/10.1016/j.matt.2020.07.019>

tunneling current through the nanogap was used to distinguish the trapping states of the target single molecule. On the other hand, single-molecule plasmonic optical trapping brings new opportunities to the field of molecular electronics,<sup>44–47</sup> such as constructing optically controlled single-molecule junction and increasing the detection efficiency. By changing the wavelength, polarization, and intensity of the incident light, we proved that the SP-enhanced electromagnetic field plays a critical role in the single-molecule trapping, which was also supported by theoretical simulations of the electromagnetic field, local heating, and optical forces generated by SPs. Benefiting from the localized enhancement of the electromagnetic field by SPs, single-molecule trapping can be performed under non-focused illumination (50 mW,  $\sim 10^6$  W/m<sup>2</sup>), in contrast to conventional optical trapping systems ( $10^9$ – $10^{12}$  W/m<sup>2</sup>). Moreover, the SP-based trapping effect is universal for other molecules and even can be further applied for selective single-molecule trapping.

## RESULTS

### Single-Molecule Plasmonic Optical Trapping

As shown in Figure 1C, the experimental setup includes the application of an optical trapping force to trap a single molecule in solution and the use of a tunneling current to distinguish the trapping states of the target molecules (Figure S3).<sup>48–50</sup> To generate a large electromagnetic field and gain sufficient trapping force for single-molecule manipulation, we placed two gold tips in proximity to form a nanogap with an adjustable size of 0–3 nm.<sup>51–54</sup> In addition, the current through the nanotips was measured under ambient conditions using a lab-built current-voltage converter with a sensitivity of 1 pA and a sampling rate of 30 kHz. During the measurement, the two electrodes were repeatedly moved together and apart with a sub-angstrom resolution in the solution containing the target molecules by controlling the movement of the underlying piezo stacks.<sup>50</sup> When a molecule is picked up by the nanotips, the molecule bridges the separated electrodes to form a Au-molecule-Au junction. A discernible plateau can then be observed in the recorded conductance-distance traces,<sup>55</sup> which can be used to distinguish single-molecule trapping events within the nanogap. Moreover, the formation probability of molecular junction can be calculated from the distribution of plateau length,<sup>42,56</sup> which provides an indicator to show whether the SPs' effects induce the molecular trapping.

To investigate the effect of illumination on the single-molecule trapping probability, we chose OPE3-SMe (1,4-bis((4-(methylthio)phenyl)ethynyl)benzene) was chosen as a model molecule (Supplemental Information and Figure S4), as OPE3-SMe does not absorb the selected laser (Figure S5) and its conductance remains constant under illumination.<sup>57</sup> Moreover, there is no chemisorption between it and the gold surface. Thus it is difficult to be trapped by other methods. Figure 2A displays typical conductance-distance traces recorded by a lab-built mechanically controllable break junction (MCBJ) with 100-mV bias. The curves show clear steps at integer multiples of  $G_0 = 2 \times 10^2/h$ , i.e., the fundamental quantum conductance.<sup>40,41</sup> Without the probe molecule, an abrupt conductance decrease over several orders of magnitude appeared during the stretching process of the two nanotips and no conductance plateau was observed in the range lower than 1  $G_0$  (Figure 2A, black). With probe molecules (Figure 2A, gray), some conductance traces show well-defined plateaus in the range of  $10^{-4}$  to  $10^{-5}$   $G_0$ , suggesting the formation of single-molecule junctions between the two gold tips. Under illumination, the conductance plateaus of the molecular junctions appear in a similar range (Figure 2A, green and orange). For all experiments, thousands of individual traces were recorded, and the corresponding all-data-point two-dimensional (2D) conductance-distance histograms

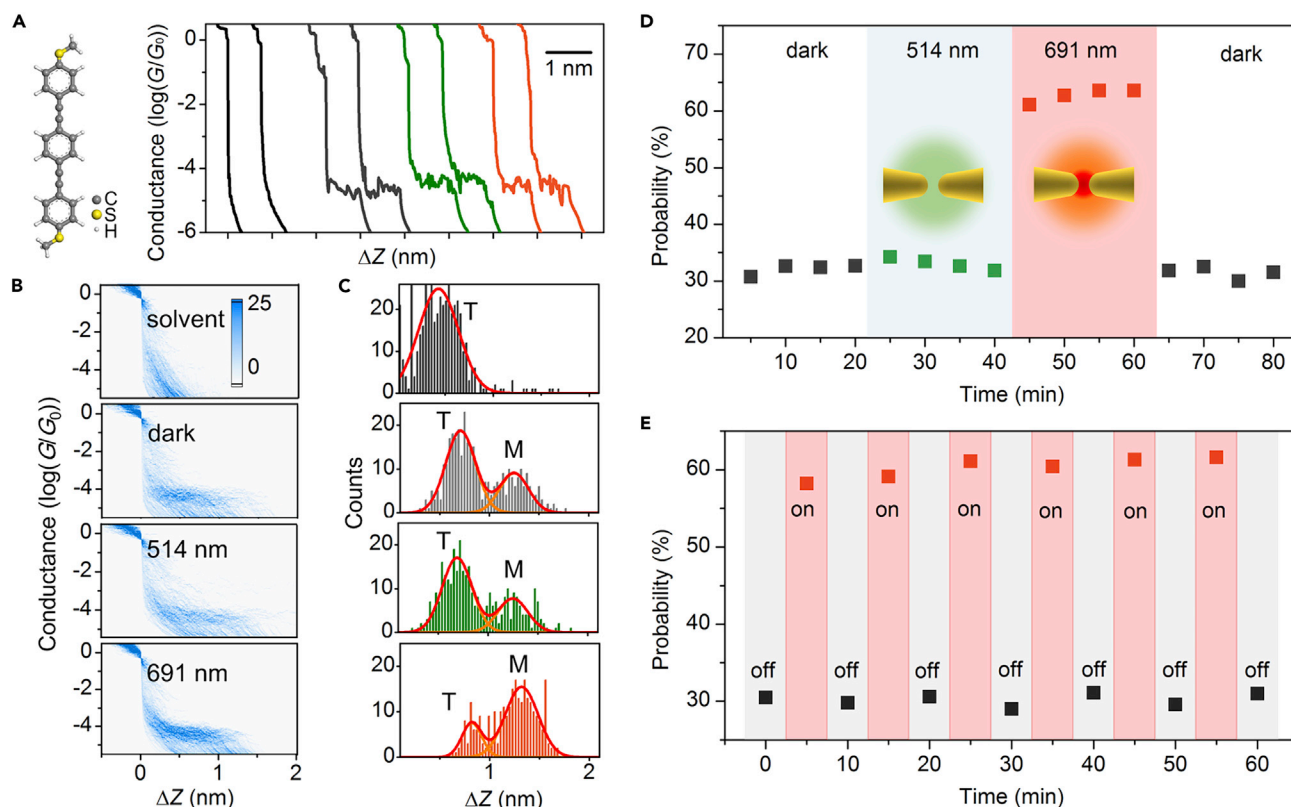


**Figure 2. Detection of the Single-Molecule Trapping and Release**

(A) Typical individual conductance-distance traces from break junction measurements of OPE-SMe molecules, where black represents the solvent without the probe molecule, gray represents OPE3-SMe without illumination, green represents OPE3-SMe under 514-nm illumination, and orange represents OPE3-SMe under 691-nm illumination. Two typical individual traces are shown for every condition.

(B) 2D conductance-distance histograms of OPE3-SM measured under different conditions.

(C) Relative displacement distributions of conductance-distance traces from the measurements corresponding to (B). Gaussian fitting is used to find the probability of molecular junction formation, where the peak marked T comes from the tunneling traces and that marked M is from the molecular junction traces.

(D) Wavelength-controlled single-molecule trapping.

(E) Single-molecule trapping and release under chopped incident light (691 nm), which shows high repeatability. The concentration of OPE3-SMe molecules is 0.001 mM. Displacement distributions were determined from  $10^{-0.3}$  to  $10^{-6} G_0$ .

were constructed to extract statistical results (Figure 2B). Without the probe molecule, the histogram shows no conductance cloud below  $1 G_0$ . When the probe molecule was added, a conductance cloud emerged at approximately  $10^{-4}$  to  $10^{-5} G_0$ , which is consistent with the previous report.<sup>57</sup> The probable single-molecule conductance remained constant in all measurements, which was also further supported by the one-dimensional (1D) conductance histograms (Figure S6). However, under 691-nm laser illumination the cloud becomes more pronounced, consistent with the increased intensity of molecule conductance in 1D conductance histograms (Figure S6), compared with that without illumination or with 514-nm laser illumination, which suggests that the formation probability of the molecular junction increased.

The single-molecule trapping probability can be quantitatively determined from the relative displacement distribution.<sup>42,56</sup> In addition to the solvent experiment, where a single peak represents the tunneling current through the solvent within the nanogap (T in Figure 2C), two peaks appeared in the displacement distribution in the



presence of target molecules (T and M). Thus, the single-molecule trapping probability can be determined from the peak area ratio of the molecular junction peak (M) (Figure 2C). Without illumination, the formation probability is approximately 30%, which represents the background probability to pick up a molecule ( $P_0$ ). This probability is mainly based on the free diffusion of molecules and the interaction between the molecule and electrode. When exposed to 691-nm laser, the formation probability improved to 65%, indicating it became easier for the nanotips to pick up a single molecule. Moreover, the minor effect on the trapping probability under 514-nm illumination demonstrates that the trapping probability depends on the wavelength of the incident light, suggesting that the trapping effect is driven by the SPs' effect. The incident light in the SP region leads to significant localized electromagnetic enhancement; in contrast, the enhancement at the interband transition region of gold is limited.<sup>52,54,58</sup>

Next, we carried out real-time single-molecule trapping and release by lasers with different wavelengths (Figures S7 and S8) and the chopped 691-nm laser (Figures S9–S11). Figure 2D shows the wavelength-controlled single-molecule trapping and release. Similar to the steady-state experiments, the formation probability of a single-molecule junction does not change under 514-nm illumination. When the incident light was adjusted from 514 nm to 691 nm, the trapping probability increased from ~30% to over 60%. When the incident light was switched off, the formation probability reverted to the initial state, which indicates the release of the trapped molecule. Figure 2E demonstrates continuous trapping and release cycles whereby the trapping probability remains constant without any attenuation after six cycles lasting for more than 60 min, suggesting the trapping and release of a single molecule were highly reversible, reproducible, and robust.

### Theoretical Calculation of the Electromagnetic Field and Optical Force

To reveal the driving force of the single-molecule trapping and release, we simulated the photothermal effect, electromagnetic field, and optical forces generated by SPs by using the finite element method.<sup>23,52,59</sup> As the quantized conductance steps occurring at integer multiples of  $G_0$  suggest the atomic shape of the gold electrodes, we constructed a calculation model with 0.25-nm surface roughness (details are shown in section 5 of Supplemental Information, Table S1, and Figure S12, and the roles of surface roughness and gap size are also discussed in Figures S20–S22).<sup>53</sup> Firstly, the calculated plasmonic spectra of the coupled nanotips showed a resonance at about 680 nm (Figures S13 and S14), which agreed well with the trapping effect observed under 691-nm illumination. We then calculated the photothermal effect under 514-nm and 691-nm illumination. This revealed that the temperature increases near the electrodes are both negligible (<0.2 K, Figure S15), demonstrating that a photothermal effect is not responsible for the molecular trapping. Figure 3A displays the spatial distribution of the electromagnetic field around the gold tips under 691-nm illumination with horizontal polarization. An electromagnetic hotspot is located in the nanogap, with a large field enhancement approaching 2,000. As shown in Figures 3B and 3C, within the hotspot region the electromagnetic gradient generates an optical force as large as several piconewtons, which is able to overcome thermal fluctuations ( $kT$ ) and thus enables the optical trapping of single molecules at room temperature, consistent with previous theoretical reports (Table S2).<sup>22–24</sup> The optical force vector shown in Figure 3D further confirms the force flow and the optical trapping, where the molecules in the vicinity of the nanogap are attracted to the hotspot region, increasing the formation probability of the molecular junction (Figure S16). We further introduced the trapping potential ( $U$ ) to describe the decreased energy due to the interaction of the optical field (details

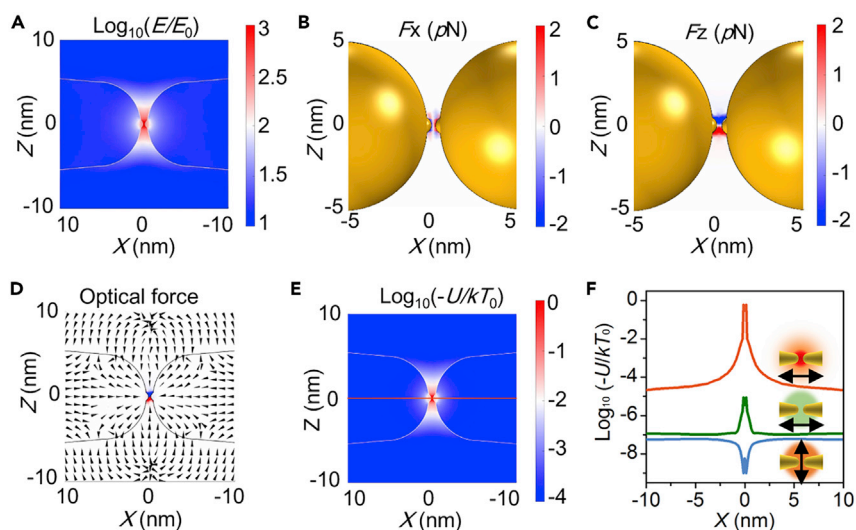


**Figure 3. Theoretical Calculation of the Electromagnetic Field and Optical Force under Illumination (Front View, X-Z Plane)**

(A) Spatial distribution of the logarithm of the electric field enhancement.

(B) The X component of the gradient forces (in the polarization direction) shows a negative force (from +X to -X) on the left side of the hot spot and a positive force on the right side, which indicates that the molecules tend to move to the surface of the tip.

(C) The Z component of the gradient forces shows a negative force (from +Z to -Z) at the top of the hot spot and a positive force at the bottom, which indicates that molecules will be drawn inside the hot spot.

(D) Mapping of the optical force vector, which shows that molecules in the vicinity of the junction will be attracted to the hot spot due to the gradient force. The intensity is normalized to show the complete vector flow.

(E) Spatial distribution of the trapping potential ( $U$ ) in units of  $kT_0$  ( $T_0 = 300$  K), under 691-nm laser illumination.

(F) Calculated trapping potential along the red line shown in (E) under light of different wavelengths and different polarizations to the nanotip couple, specifically, 691 nm with horizontal polarization (red line), 514 nm with horizontal polarization (black line), and 691 nm with vertical polarization (blue line). The insets give the top view of the nanotips and the polarization of the incident light.

are shown in Section 5.2 of [Supplemental Information](#) and [Figure S17](#)). [Figure 3E](#) shows the spatial distribution of the trapping potential in units of  $kT_0$ , where  $k$  is Boltzmann's constant and  $T_0$  is  $\sim 300$  K. Based on the Boltzmann distribution, the enhancement of trapping probability can be described as  $E_p = \exp(-U/kT_0)$ . The trapping probability ( $P$ ) can be described as  $E_p \cdot P_0 = P_0 \exp(-U/kT_0)$ , where  $U$  is linear with the light intensity. Under 691-nm laser illumination, the trapping potential is approximately  $-0.6 kT_0$ , and thus the trapping probability can be improved by approximately 2-fold, which agrees well with the experimental result, i.e., the enhancement of trapping probability from about 30% to 60%. In contrast, a limited electromagnetic enhancement is found under 514-nm laser illumination, which lies in the interband transition region of gold nanotips. The amplitude decreased considerably, which is consistent with the unchanged trapping probability in experiments (see [Figure S18](#) for details). The calculation also demonstrates that incident light with vertical polarization would provide a small negative potential in the gap, which cannot improve the molecular trapping ([Figures 3F](#) and [S19](#)).

### Single-Molecule Trapping and Release Depending on the Laser Polarization and Intensity

To further validate the SP-induced trapping effect, we performed single-molecule trapping experiments under the incident light (691 nm) with different polarizations,

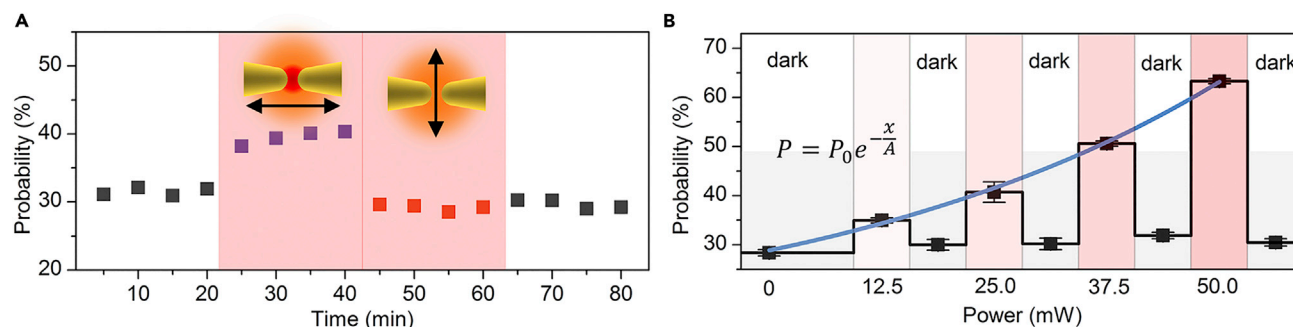


**Figure 4. Single-Molecule Trapping and Release by Varying the Laser Polarization and Intensity**

(A) Polarization-controlled single-molecule trapping and release. The black arrows represent the polarization of the incident light.

(B) Trapping probability as a function of the laser intensity (691 nm). This can be well fitted with a single exponential function, where  $P_0$  and  $A$  are constants, and  $P_0$  is the trapping probability without illumination. The error bars represent the relative deviation.

as shown in Figure 4A (the laser power is 25 mW, see Section 6 in Supplemental Information and Figures S23 and S24). The incident light with horizontal polarization to the nanotip couple significantly improved the formation probability of the molecular junction from 30% to 45%. In contrast, under illumination with vertical polarization, the formation probability of the molecular junction was similar to that without illumination, which agrees well with the calculations. These results further proved that the trapping effect was mainly from SPs. Figure 4B shows the trapping probability as a function of the laser intensity, which can be fitted with a single exponential function. The excellent fitting of the experimental data to the derived equations in theory supports our conclusion that the trapping force originates from the enhanced local electromagnetic field of SPs (Supplemental Information; Figures S25 and S26). Similar trapping and release phenomena were observed in experiments with different molecules (Supplemental Information; for more details, see Figures S27–S33), suggesting that the SP-induced trapping effect is universal for different molecules.

### Single-Molecule Plasmonic Optical Trapping for Selective Single-Molecule Trapping

Theoretically, the optical trapping force is decided by the molecular polarizability, which is highly related to the molecular volume (see Section 5 in the Supplemental Information for more details). Generally, for molecules with similar structures, the larger size would lead to a larger polarizability. Thus, this specificity can be exploited to achieve a trapping selectivity for different molecular sizes. To demonstrate the potential of our method for selective molecular trapping, we investigated two molecules with different lengths and the same anchoring groups (Figure 5A; Section 8 in Supplemental Information; Figures S34–S37). Figure 5B shows the schematic of selective single-molecule optical trapping. If the optical force can only trap one molecule of the two, the formation probability of the molecular junction will increase selectively. Figures 5C and 5D show the all-data-point 2D conductance-distance histograms without and with 691-nm illumination. Under illumination, the conductance cloud of OPE3-SMe (the cloud emerged in the range of  $10^{-4}$  to  $10^{-5}$   $G_0$ ) became more pronounced, while the intensity of the conductance cloud of OPE2-SMe (the cloud emerged in the range of  $10^{-3}$  to  $10^{-4}$   $G_0$ ) showed no change, even with a slight decrease. These findings indicated the selective increase of single-molecule trapping probability, which is further proved by the 1D conductance histograms (Figures 5E and S37). Quantitatively, the relative formation probability of OPE3-SMe junction over OPE2-SMe junction increased from 52% to 80% under 691-nm illumination



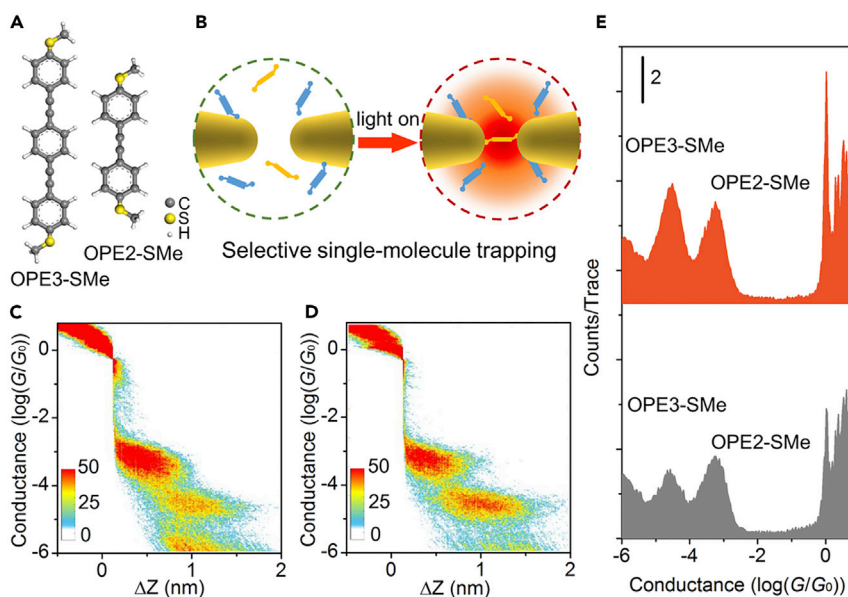


**Figure 5. Selective Single-Molecule Trapping**

(A) Structures of the OPE3-SMe (~2 nm) and OPE2-SMe (~1.5 nm) that were used for the selective trapping experiment.

(B) Schematic of selective single-molecule plasmonic optical trapping.

(C) 2D conductance-distance histograms in dark conditions.

(D) 2D conductance-distance histograms under 691-nm illumination.

(E) 1D conductance histograms of the mixed solution including OPE2-SMe and OPE3-SMe in dark conditions (gray) and under 691-nm illumination (orange).

(details are shown in Section 8 of [Supplemental Information](#) and [Table S3](#)). This experiment not only shows the capability of our method in selective single-molecule trapping but also proves that the optical forces make the main contribution to the trapping event.

## DISCUSSION

This single-molecule plasmonic optical trapping technique provides the first demonstration that a free single molecule of ~2 nm can be directly trapped and released in solution using a plasmonic optical nanogap, pushing the volume of a free object that can be manipulated in solution down to an unprecedented 2 nm. Comprehensive experiments and theoretical calculations revealed that the trapping force originates from the enhanced localized electromagnetic field generated by plasmonic nanomaterials. This SP-induced mass transport also brings further insight to plasmonic applications, e.g., sensors, enhanced spectroscopy, and chemistry, as well as molecular electronics. It offers an approach for the controllable trapping of single molecules or other objects in the size range of primary interest to physics, chemistry, and nanotechnology life and material sciences without the limitations of strong bonding group, UHV, and ultra-low temperature, thus assisting explorations at the single-molecule level, for example, investigating molecule-protein interactions, controlling single-molecule reactions, or constructing nanodevices and molecular machines.

## EXPERIMENTAL PROCEDURES

### Resource Availability

#### Lead Contact

Further information and requests for resources and reagents should be directed to and will be fulfilled by the Lead Contact, Prof. Zhong-Qun Tian ([zqtian@xmu.edu.cn](mailto:zqtian@xmu.edu.cn)).

### Materials Availability

This study did not generate new unique reagents.

### Data and Code Availability

All data supporting the main findings of the paper are available within the main paper and its [Supplemental Information](#) files and from the Lead Contact upon reasonable request.

### Experimental

The single-molecule trapping was performed by the home-built setup combined with light control component and single-molecule detection system. The light control component consists of lasers with different wavelengths, reflector, polarizer, and chopper. Single-molecule measurements were performed using a home-built MCBJ setup. For single-molecule trapping, a coupling of two gold nanotips supplying extremely strong electric field enhancement was used as the single-molecule tweezers; meanwhile they were used as the electrodes of the MCBJ setup to distinguish the trapping state of the single molecule. The test-molecule solution (0.001 mM in mixture solvent of tetrahydrofuran/mesitylene 1:4) was pumped into the liquid cell (100  $\mu$ L). During the measurement, the molecule can be picked up by the tips to form the Au-molecule-Au junction. The entire traces, as acquired during the opening and closing process, were recorded for further data analysis. The above cycle was repeated about 1,000 times at each set of experimental conditions. In data processing for constructing the conductance histogram, the total counts at each condition were normalized by 1,000 traces unless otherwise noted. The complete data analysis is based on a lab-developed program (WA-BJ code), which runs under LabVIEW 2011.

### Theoretical

The simulation of optical forces is performed using commercial finite elements method software COMSOL Multiphysics. The single molecule is considered as a point-like dipole with isotropic dipolar polarizability  $\alpha(\omega) = \alpha'(\omega) + i\alpha''(\omega)$ . The polarizability  $\alpha$  is a parameter describing the induced electronic dipolar transition from the highest occupied to lowest unoccupied molecular orbitals, and thus is related to transition strength. In this case, the optical force  $F$  upon molecules is the sum of gradient force  $F_g = 0.5\alpha'\nabla|E|^2$  and scattering force  $F_s = 0.5k\alpha''\nabla|E|^2$ , where  $E$  is the electric field and  $k$  is wave vector. A stable trap requires that gradient forces should be much greater than scattering force. In our experiments, we choose non-resonant molecules ( $\alpha' \gg \alpha''$ ) to ensure a minor contribution from scattering force. The other criterion for stable trapping is that the trapping forces must be greater than Brownian motion forces to beat the thermal fluctuation. Since the gradient force is a conserve force, one can introduce a trapping potential  $U = -0.5\alpha'|E|^2$  to describe the decreased energy due to the interaction of optical field. By introducing trapping potential, we can directly compare the trapping potential  $U$  with thermal fluctuation energy  $kT_0$ , and the enhanced probability of trapping molecules is written as  $E_p = P/P_0 = \exp(-U/kT_0)$ , where  $k$  is the Boltzmann constant and  $T_0$  is the temperature (300 K).  $P_0$  is the trapping probability without illumination. Thus the trapping probability under illumination can be expressed as  $P = P_0 \exp(-U/kT_0)$ . So a single exponential function can be used to express the relationship between the trapping probability and light intensity,  $P = P_0 \exp(0.5\alpha'|E|^2/kT_0)$ . It should be emphasized that if the molecule is completely free,  $P_0$  is mainly related to the molecular concentration. While even without chemical adsorption, molecules often interact with metal surfaces. So we believe that  $P_0$  is also related to the interaction between the molecule

and metal surface, such as the adsorption effect, in single-molecule plasmonic optical trapping.

### SUPPLEMENTAL INFORMATION

Supplemental Information can be found online at <https://doi.org/10.1016/j.matt.2020.07.019>.

### ACKNOWLEDGMENTS

This work is financially supported by the National Natural Science Foundation of China (21533006, 21621091, 21673195, 21973079, and 21722305), and the National Key R&D Program (2017YFA0204902, 2015CB932300). The authors thank Bin Ren, Zhao-Xiong Xie, Nan-Feng Zheng, Su-Yuan Xie, Hai-Ping Xia, Jian-Feng Li, and Xia-Guang Zhang for fruitful discussions, and Liang Chen, Shu Hu, and Zhi-Chao Lei for help in experiments.

### AUTHOR CONTRIBUTIONS

Z.-Q.T., W.H., and Y.Y. co-supervised the project. C.Z. conceived the ideas and designed the experiments. C.Z. and G.W. performed the experiments. J.Y. carried out the calculations. C.Z. prepared the first draft of the paper. All authors contributed to data interpretation and writing of the manuscript.

### DECLARATION OF INTERESTS

The authors declare no competing financial interests.

Received: April 13, 2020

Revised: June 19, 2020

Accepted: July 10, 2020

Published: August 12, 2020

### REFERENCES

- Ashkin, A. (1970). Acceleration and trapping of particles by radiation pressure. *Phys. Rev. Lett.* **24**, 156–159.
- Ashkin, A., Dziedzic, J.M., Bjorkholm, J.E., and Chu, S. (1986). Observation of a single-beam gradient force optical trap for dielectric particles. *Opt. Lett.* **11**, 288–290.
- Mehta, A.D., Rief, M., Spudich, J.A., Smith, D.A., and Simmons, R.M. (1999). Single-molecule biomechanics with optical methods. *Science* **283**, 1689–1695.
- Abbondanzieri, E.A., Greenleaf, W.J., Shaevitz, J.W., Landick, R., and Block, S.M. (2005). Direct observation of base-pair stepping by RNA polymerase. *Nature* **438**, 460–465.
- Liu, C., Kubo, K., Wang, E., Han, K.-S., Yang, F., Chen, G., Escobedo, F.A., Coates, G.W., and Chen, P. (2017). Single polymer growth dynamics. *Science* **358**, 352–355.
- Neuman, K.C., and Nagy, A. (2008). Single-molecule force spectroscopy: optical tweezers, magnetic tweezers and atomic force microscopy. *Nat. Methods* **5**, 491–505.
- Lee, H.J., and Ho, W. (1999). Single-bond formation and characterization with a scanning tunneling microscope. *Science* **286**, 1719–1722.
- Pavliček, N., and Gross, L. (2017). Generation, manipulation and characterization of molecules by atomic force microscopy. *Nat. Rev. Chem.* **1**, <https://doi.org/10.1038/s41570-016-0005>.
- Chu, S. (1998). Nobel Lecture: the manipulation of neutral particles. *Rev. Mod. Phys.* **70**, 685–706.
- Liu, L.R., Hood, J.D., Yu, Y., Zhang, J.T., Hutzler, N.R., Rosenband, T., and Ni, K.-K. (2018). Building one molecule from a reservoir of two atoms. *Science* **360**, 900–903.
- Viteau, M., Chotia, A., Allegrini, M., Bouloufa, N., Dulieu, O., Comparat, D., and Pillet, P. (2008). Optical pumping and vibrational cooling of molecules. *Science* **321**, 232–234.
- Shuman, E.S., Barry, J.F., and DeMille, D. (2010). Laser cooling of a diatomic molecule. *Nature* **467**, 820–823.
- Fields, A.P., and Cohen, A.E. (2011). Electrokinetic trapping at the one nanometer limit. *Proc. Natl. Acad. Sci. U S A* **108**, 8937–8942.
- Wang, Q., Goldsmith, R.H., Jiang, Y., Bockenhauer, S., and Moerner, W.E. (2012). Probing single biomolecules in solution using the anti-brownian electrokinetic (ABEL) trap. *Acc. Chem. Res.* **45**, 1955–1964.
- Ashkin, A., Dziedzic, J.M., and Yamane, T. (1987). Optical trapping and manipulation of single cells using infrared laser beams. *Nature* **330**, 769–771.
- Block, S.M., Goldstein, L.S.B., and Schnapp, B.J. (1990). Bead movement by single kinesin molecules studied with optical tweezers. *Nature* **348**, 348–352.
- Kuo, S., and Sheetz, M. (1993). Force of single kinesin molecules measured with optical tweezers. *Science* **260**, 232–234.
- Svoboda, K., Schmidt, C.F., Schnapp, B.J., and Block, S.M. (1993). Direct observation of kinesin stepping by optical trapping interferometry. *Nature* **365**, 721–727.
- Grier, D.G. (2003). A revolution in optical manipulation. *Nature* **424**, 810–816.
- Juan, M.L., Righini, M., and Quidant, R. (2011). Plasmon nano-optical tweezers. *Nat. Photon.* **5**, 349–356.
- Maragò, O.M., Jones, P.H., Gucciarini, P.G., Volpe, G., and Ferrari, A.C. (2013). Optical trapping and manipulation of nanostructures. *Nat. Nanotech.* **8**, 807–819.

22. Novotny, L., Bian, R.X., and Xie, X.S. (1997). Theory of nanometric optical tweezers. *Phys. Rev. Lett.* **79**, 645–648.
23. Xu, H., and Käll, M. (2002). Surface-plasmon-enhanced optical forces in silver nanoaggregates. *Phys. Rev. Lett.* **89**, 246802.
24. Calander, N., and Willander, M. (2002). Optical trapping of single fluorescent molecules at the detection spots of nanoprobe. *Phys. Rev. Lett.* **89**, 143603.
25. Volpe, G., Quidant, R., Badenes, G., and Petrov, D. (2006). Surface plasmon radiation forces. *Phys. Rev. Lett.* **96**, 238101.
26. Righini, M., Zelenina, A.S., Girard, C., and Quidant, R. (2007). Parallel and selective trapping in a patterned plasmonic landscape. *Nat. Phys.* **3**, 477–480.
27. Grigorenko, A.N., Roberts, N.W., Dickinson, M.R., and Zhang, Y. (2008). Nanometric optical tweezers based on nanostructured substrates. *Nat. Photon.* **2**, 365–370.
28. Koya, A.N., Cunha, J., Guo, T., Toma, A., Garoli, D., Wang, T., Juodkakis, S., Cojoc, D., and Zaccaria, R.P. (2020). Novel plasmonic nanocavities for optical trapping-assisted biosensing applications. *Adv. Opt. Mater.* **8**, 1901481.
29. Hansen, P.M., Bhatia, V.K., Harrit, N., and Oddershede, L. (2005). Expanding the optical trapping range of gold nanoparticles. *Nano Lett.* **5**, 1937–1942.
30. Lehmuskero, A., Johansson, P., Rubinsztein-Dunlop, H., Tong, L., and Käll, M. (2015). Laser trapping of colloidal metal nanoparticles. *ACS Nano* **9**, 3453–3469.
31. Lin, L., Wang, M., Peng, X., Lissek, E.N., Mao, Z., Scarabelli, L., Adkins, E., Coskun, S., Unalan, H.E., Korgel, B.A., et al. (2018). Opto-thermoelectric nanotweezers. *Nat. Photon.* **12**, 195–201.
32. Righini, M., Volpe, G., Girard, C., Petrov, D., and Quidant, R. (2008). Surface plasmon optical tweezers: tunable optical manipulation in the femtonewton range. *Phys. Rev. Lett.* **100**, 186804.
33. Pang, Y., and Gordon, R. (2012). Optical trapping of a single protein. *Nano Lett.* **12**, 402–406.
34. Yoo, D., Kargal Iaxminarayana, G., Choi, H.-K., Mohr, D.A., Ertsgaard, C.T., Gordon, R., and Oh, S.-H. (2018). Low-power optical trapping of nanoparticles and proteins with resonant coaxial nanoaperture using 10 nm gap. *Nano Lett.* **18**, 3637–3642.
35. Zhao, Y., Saleh, A.A.E., van de Haar, M.A., Baum, B., Briggs, J.A., Lay, A., Reyes-Becerra, O.A., and Dionne, J.A. (2017). Nanoscopic control and quantification of enantioselective optical forces. *Nat. Nanotech.* **12**, 1055–1059.
36. Shao, L., Yang, Z.-J., Andren, D., Johansson, P., and Käll, M. (2015). Gold nanorod rotary motors driven by resonant light scattering. *ACS Nano* **9**, 12542–12551.
37. Huang, J., Mousavi, M.Z., Zhao, Y., Hubarevich, A., Omeis, F., Giovannini, G., Schutte, M., Garoli, D., and De, A.F. (2019). SERS discrimination of single DNA bases in single oligonucleotides by electro-plasmonic trapping. *Nat. Commun.* **10**, 1–10.
38. Kitahama, Y., Funaoka, M., and Ozaki, Y. (2019). Plasmon-enhanced optical tweezers for single molecules on and near a colloidal silver nanoaggregate. *J. Phys. Chem. C* **123**, 18001–18006.
39. Saleh, A.A.E., and Dionne, J.A. (2012). Toward efficient optical trapping of sub-10-nm particles with coaxial plasmonic apertures. *Nano Lett.* **12**, 5581–5586.
40. Quek, S.Y., Kamenetska, M., Steigerwald, M.L., Choi, H.J., Louie, S.G., Hybertsen, M.S., Neaton, J.B., and Venkataraman, L. (2009). Mechanically controlled binary conductance switching of a single-molecule junction. *Nat. Nanotech.* **4**, 230–234.
41. Hong, W., Manrique, D.Z., Moreno-Garcia, P., Gulcur, M., Mishchenko, A., Lambert, C.J., Bryce, M.R., and Wandlowski, T. (2012). Single molecular conductance of tolanes: experimental and theoretical study on the junction evolution dependent on the anchoring group. *J. Am. Chem. Soc.* **134**, 2292–2304.
42. Huang, C., Jevric, M., Borges, A., Olsen, S.T., Hamill, J.M., Zheng, J.-T., Yang, Y., Rudnev, A., Baghernejad, M., Broekmann, P., et al. (2017). Single-molecule detection of dihydroazulene photo-thermal reaction using break junction technique. *Nat. Commun.* **8**, 15436.
43. Lumbroso, O.S., Simine, L., Nitzan, A., Segal, D., and Tal, O. (2018). Electronic noise due to temperature differences in atomic-scale junctions. *Nature* **562**, 240–244.
44. Xiang, D., Wang, X., Jia, C., Lee, T., and Guo, X. (2016). Molecular-scale electronics: from concept to function. *Chem. Rev.* **116**, 4318–4440.
45. Sun, L., Diazfernandez, Y.A., Gschneidnet, T., Westerlund, F., Laraavila, S., and Mothpoulsen, K. (2014). Single-molecule electronics: from chemical design to functional devices. *Chem. Soc. Rev.* **43**, 7378–7411.
46. Xin, N., Guan, J., Zhou, C., Chen, X., Gu, C., Li, Y., Ratner, M.A., Nitzan, A., Stoddard, J.F., and Guo, X. (2019). Concepts in the design and engineering of single-molecule electronic devices. *Nat. Rev. Phys.* **1**, 211–230.
47. Gehring, P., Thijssen, J.M., and van der Zant, H.S.J. (2019). Single-molecule quantum-transport phenomena in break junctions. *Nat. Rev. Phys.* **1**, 381–396.
48. Aradhya, S.V., and Venkataraman, L. (2013). Single-molecule junctions beyond electronic transport. *Nat. Nanotech.* **8**, 399–410.
49. Tan, S.F., Wu, L., Yang, J.K.W., Bai, P., Bosman, M., and Nijhuis, C.A. (2014). Quantum plasmon resonances controlled by molecular tunnel junctions. *Science* **343**, 1496–1499.
50. Jia, C., Migliore, A., Xin, N., Huang, S., Wang, J., Yang, Q., Wang, S., Chen, H., Wang, D., Feng, B., et al. (2016). Covalently bonded single-molecule junctions with stable and reversible photoswitched conductivity. *Science* **352**, 1443–1445.
51. Nie, S., and Emory, S.R. (1997). Probing single molecules and single nanoparticles by surface-enhanced Raman scattering. *Science* **275**, 1102–1106.
52. Ding, S.-Y., Yi, J., Li, J.-F., Ren, B., Wu, D.-Y., Panneerselvam, R., and Tian, Z.-Q. (2016). Nanostructure-based plasmon-enhanced Raman spectroscopy for surface analysis of materials. *Nat. Rev. Mater.* **1**, 16021.
53. Benz, F., Schmidt, M.K., Dreismann, A., Chikkaraddy, R., Zhang, Y., Demetriadou, A., Carnegie, C., Ohadi, H., de Nijs, B., Esteban, R., et al. (2016). Single-molecule optomechanics in “picocavities”. *Science* **354**, 726–729.
54. Baumberg, J.J., Aizpurua, J., Mikkelsen, M.H., and Smith, D.R. (2019). Extreme nanophotonics from ultrathin metallic gaps. *Nat. Mater.* **18**, 668–678.
55. Xu, B., and Tao, N.J. (2003). Measurement of single-molecule resistance by repeated formation of molecular junctions. *Science* **301**, 1221–1223.
56. Guan, J., Jia, C., Li, Y., Liu, Z., Wang, J., Yang, Z., Gu, C., Su, D., Houk, K.N., Zhang, D., and Guo, X. (2018). Direct single-molecule dynamic detection of chemical reactions. *Sci. Adv.* **4**, earr2177.
57. Frisenda, R., Tarkuç, S., Galán, E., Perrin, M.L., Eelkema, R., Grozema, F.C., and van der Zant, H.S.J. (2015). Electrical properties and mechanical stability of anchoring groups for single-molecule electronics. *Beilstein J. Nanotech.* **6**, 1558–1567.
58. Zheng, B.Y., Zhao, H., Manjavacas, A., McClain, M., Nordlander, P., and Halas, N.J. (2015). Distinguishing between plasmon-induced and photoexcited carriers in a device geometry. *Nat. Commun.* **6**, 7797.
59. Baffou, G., Quidant, R., and Girard, C. (2010). Thermoplasmonics modeling: a Green’s function approach. *Phys. Rev. B* **82**, 165424.